Stereochemical Investigation of Three 47-Electron Carbonyl, Nitrene Bicapped Trimetal Clusters in the Homologous 48/47-Electron $[Co_3(\eta^5\text{-}C_5Me_5)_{3-x}(\eta^5\text{-}C_5H_4Me)_x(\mu_3\text{-}CO)(\mu_3\text{-}NH)]^n$ Series (x = 0, 1, 2; n = 0, +1): Bonding Analysis of the Redox-Generated Changes in Geometry upon Formation of Electron-Deficient Species by Oxidation of Triangularly Bonded 48-Electron Metal Clusters Containing π-Acceptor Carbonyl Capping Ligands

Michael S. Ziebarth[1] and Lawrence F. Dahl*

Contribution from the Department of Chemistry, University of Wisconsin—Madison, Madison, Wisconsin 53706. *Received September 7, 1989*

Abstract: The isolation and stereochemical characterization of three 47-electron triangular metal monocations, $[Co_3Cp^*_{3-x}Cp'_x(\mu_3\text{-}CO)(\mu_3\text{-}NH)]^+$ [where x = 0 (**1**$^+$); x = 1 (**2**$^+$); x = 2 (**3**$^+$); Cp* and Cp′ denote η^5-C_5Me_5 and η^5-C_5H_4Me, respectively], with capping CO and NH ligands are reported. Structural analyses of these electron-deficient cation radicals containing $Co_3(CO)(NH)$ cores were carried out in order to determine for the first time the changes in geometry caused by the removal of a valence electron from a completely bonding (48-electron) triangular metal cluster. Mixed Cp* and Cp′ ligands were utilized not only to minimize the possibility of an averaged structure resulting from a 3-fold crystallographic disorder of the triangular metal cluster but also to probe the different electronic and steric effects of these terminal ligands. Reaction of trimethylsilyl azide with $CoCp^*(CO)_2$ and $CoCp'(CO)_2$ produced the four desired 48-electron mixed Cp*/Cp′ tricobalt clusters, $Co_3Cp^*_{3-x}Cp'_x(\mu_3\text{-}CO)(\mu_3\text{-}NR)$ [where R = H: x = 1 (**2**); x = 2 (**3**); and where R = $SiMe_3$: x = 1 (**2a**); x = 2 (**3a**)]. Oxidations with $AgPF_6$ of the previously reported $Co_3Cp^*_3(\mu_3\text{-}CO)(\mu_3\text{-}NH)$ (**1**) and of the OC, HN bicapped **2** and **3** gave quantitative yields of the 47-electron **1**$^+$, **2**$^+$, and **3**$^+$, respectively. Analogous oxidations of the corresponding OC, Me_3SiN bicapped **2a** and **3a** also produced **2**$^+$ and **3**$^+$ via cleavage of the N–$SiMe_3$ bond and concomitant protonation. X-ray crystallographic determinations of the three 47-electron **1**$^+$, **2**$^+$, and **3**$^+$ and of the 48-electron **3** allowed a comparative geometrical analysis of their $Co_3(CO)(NH)$ cores as well as that of the structurally known **1**. Removal of an electron from the 48-electron **1**, which has three Cp* ligands, results in a *shortening* of the mean Co–Co and mean Cp*Co–NH distances by identical values of only 0.019 Å and a simultaneous *lengthening* of the mean Cp*Co–CO distance by 0.049 Å. The much larger change in the mean Cp*Co–CO bond length can be ascribed to the dominating effect of the "net" destabilization of the much stronger trimetal–carbonyl interactions due to less Cp*Co–CO π back-bonding in **1**$^+$, which effectively counterbalances a "net" stabilization of the relatively weak metal–metal interactions and thereby opposes any decrease in the Co–Co distances. Although oxidation of **1** to **1**$^+$ was shown from preliminary MO calculations with the Fenske–Hall model to correspond to an electron removal from two filled doubly degenerate e HOMOs under assumed C_{3v} symmetry, no geometrical deformation of the $Co_3(CO)(NH)$ core in the 47-electron **1**$^+$ from C_{3v} to C_s symmetry is observed; the Co–Co bond lengths are within 0.022 Å of one another, and there are no pronounced variations in the individual Cp*Co–CO or Cp*Co–NH bond lengths, which are within 0.015 and 0.008 Å, respectively, of their mean values. These results suggest that the Jahn–Teller effect in **1**$^+$ either is distributed over the entire monocation instead of being concentrated in a particular part of the $Co_3(CO)(NH)$ core or is mainly a consequence of instantaneous deformations of the Cp* ligands from the non-3-fold molecular symmetry splitting the degeneracy of the $^3/_4$-filled HOMOs. A third distinct possibility is that the $Co_3(CO)(NH)$ core of **1**$^+$ is 3-fold-disordered in the solid state even though the crystallographic site symmetry is C_1-1. The geometries of the $Co_3(CO)(NH)$ cores of **2**$^+$, which has one Cp′ and two Cp* ligands, and **3**$^+$, which contains one Cp* and two Cp′ ligands, are markedly distorted from pseudo-C_{3v} to pseudo-C_s symmetry. The observed slight change (if any) in mean metal–metal distance upon oxidation of a 48-electron cluster to the corresponding 47-electron cluster is in sharp contrast to the small but significant increases in mean metal–metal distances observed when similar 48-electron tricobalt clusters are reduced to their corresponding 49/50-electron clusters. This indicates that in known 48-electron tricobalt clusters, where the redox behavior has been investigated, the trimetal *antibonding* character is generally much less in their HOMOs than in their LUMOs. The bond-length variations stress that the metal–metal distances in the $Co_3(CO)(NH)$ cores of these 47/48-electron clusters are strongly influenced by the Cp*Co–CO and Cp′Co–CO distances, with the former being invariably smaller within a given mixed Cp*/Cp′ cluster due to greater π back-bonding from the CoCp* dπ AOs to the empty CO π*-acceptor orbitals. This qualitative bonding interpretation provides a coherent, integrated picture for electron-deficient triangular metal clusters containing capping carbonyl ligands. Its extension to the isostructural (C_{3h}-3/m averaged structure) 46-electron $Co_3Cp^*_3(\mu_3\text{-}CO)_2$ (**4**) and 46-electron $Co_3Cp_3(\mu_3\text{-}CO)_2$ (**5**) (where Cp denotes η^5-C_5H_5) provides an explanation (i.e., weaker Co–CO π back-bonding) for the 0.022-Å longer Co–CO distance in **5** as compared to that in **4**.

Systematic studies[2] in our laboratories of redox-generated variations in the geometries of metal clusters have focused on effects caused by variations of electronic configurations of a variety of metal cluster systems that function as electron-transfer reagents without rupture of their central cluster architecture. A major objective of these studies has been to interrelate and predict how

(1) Based in part on: Ziebarth, M. S. Ph.D. Thesis University of Wisconsin—Madison, Aug 1989. Present address: Washington Research Center, W. R. Grace & Co., Columbia, MD 21044.

(2) (a) For a compilation of older references, see: Reference 39 of Kharas, K. C. C.; Dahl, L. F. Ligand-Stabilized Metal Clusters: Structure, Bonding, Fluxionality, and the Metallic State. *Adv. Chem. Phys.* **1988**, *70* (part 2), 1–43. (b) Kubat-Martin, K. A.; Barr, M. E.; Spencer, B.; Dahl, L. F. *Organometallics* **1987**, *6*, 2570–2579. (c) Kubat-Martin, K. A.; Spencer, B.; Dahl, L. F. *Organometallics* **1987**, *6*, 2580–2587.

0002-7863/90/1512-2411$02.50/0

alterations in electronic structure affect metal-core geometries. These structural-bonding analyses, which may be viewed as "experimental quantum mechanics", have been useful in correlating the observed physical-chemical properties of related metal clusters.

Prior to the work reported herein, relatively few electron-deficient *homonuclear* trimetal clusters with identical terminal ligands on each metal atom have been observed. Those structurally characterized include $Co_3Cp^*_3(\mu_3\text{-}CO)_2$ (**4**).[3-5] $Co_3Cp_3(\mu_3\text{-}CO)_2$ (**5**),[6] and $Rh_3Cp^*_3(\mu_3\text{-}CO)_2$,[5,7] which are all 46-electron systems. Hence, a recent electrochemical investigation,[8,9] which showed that the 48-electron $Co_3Cp^*_3(\mu_3\text{-}CO)(\mu_3\text{-}NH)$ (**1**) has two reversible one-electron oxidations, stimulated our interest in the possibility of isolating and structurally characterizing the 47-electron monocation. It was hoped that a structural-bonding analysis of this monocation would provide insight into the nature of the HOMO in an electron-deficient metal cluster. From prior theoretical studies[3,10-12] of related triangular tricobalt systems, one would predict that the 48-electron $Co_3Cp^*_3(\mu_3\text{-}CO)(\mu_3\text{-}NH)$ should possess (under C_{3v} symmetry) four electrons in two doubly degenerate, completely filled e HOMOs of presumed trimetal antibonding orbital character. Hence, it was expected that the $Co_3(CO)(NH)$ core of its 47-electron monocation would possess a distorted C_s-type geometry with a smaller mean Co–Co distance due to a first-order Jahn–Teller effect arising from three trimetal antibonding electrons occupying the two doubly degenerate HOMOs.[13-15]

We also decided to expand our knowledge of the bonding in electron-deficient triangular metal clusters by looking at the geometrical changes due to the replacement of CoCp* fragments with CoCp′ fragments. Therefore, we synthesized and spectroscopically characterized the mixed Cp*/Cp′ 48-electron $Co_3Cp^*_{3-x}Cp'_x(\mu_3\text{-}CO)(\mu_3\text{-}NR)$ series [where R = $SiMe_3$: x = 1 (**2a**); x = 2, (**3a**); where R = H: x = 1 (**2**); x = 2 (**3**)]. X-ray crystallographic determinations of **3** and the three oxidized $[Co_3Cp^*_{3-x}Cp'_x(\mu_3\text{-}CO)(\mu_3\text{-}NH)]^+$ monocations [x = 0 ($\mathbf{1}^+$); x = 1 ($\mathbf{2}^+$); x = 2 ($\mathbf{3}^+$)] have allowed us to assess the geometrical effects of mixed Cp*/Cp′ ligands on 47-electron clusters containing a common $Co_3(CO)(NH)$ core.

A comparative structural-bonding analysis of these electron-deficient systems, which constitute the first structurally characterized 47-electron homonuclear triangular metal clusters, and of the 46-electron $Co_3Cp^*_3(\mu_3\text{-}CO)_2$ (**4**)[3-5] and $Co_3Cp_3(\mu_3\text{-}CO)_2$ (**5**)[6] has provided a self-consistent electronic rationalization of their molecular parameters. In order to highlight the geometrical differences due to the removal of an electron from the HOMOs versus the addition of an electron to the LUMOs of known 48-electron bicapped tricobalt clusters, changes in metal–metal distances upon redox formation of these 47-electron systems are compared to those determined upon redox formation of related electron-rich 49- and 50-electron triangular cobalt clusters.[16-23]

Experimental Section

General Procedures. All reactions and manipulations were carried out under purified N_2 either via standard Schlenk tube techniques or in a Vacuum Atmospheres glovebox. Solvents were dried and distilled over standard reagents and degassed before use. Infrared spectra were obtained on either a Beckman IR 4240 spectrometer or a Mattson Polaris FT-IR spectrometer, while ^1H NMR spectra were recorded on a Bruker WP-200 spectrometer.

$CoCp^*(CO)_2$ and $CoCp'(CO)_2$ were prepared according to the general method of Rausch and Genetti.[24] $Co_3Cp^*_3(\mu_3\text{-}CO)(\mu_3\text{-}NH)$ was prepared by the procedure of Bedard et al.[8] All other reagents were purchased from standard commercial sources.

Preparation of the 48-Electron $Co_3Cp^*_{3-x}Cp'_x(\mu_3\text{-}CO)(\mu_3\text{-}NR)$ Series (Where x = 1, 2; and R = H, $SiMe_3$). $CoCp^*(CO)_2$ (4.14 g, 16.6 mmol), $CoCp'(CO)_2$ (2.6 mL, 16.8 mmol), and $SiMe_3N_3$ (4.0 mL, 30.2 mmol) were dissolved in 150 mL of toluene and refluxed for 24 h. The toluene-soluble portion was filtered off, reduced in volume, and chromatographed on Al_2O_3 to separate out the first two bands—viz., the orange starting material $CoCp'(CO)_2$ and the major product, $Co_2Cp^*_2(\mu_2\text{-}CO)_2$.[25] The remaining material was eluted with CH_2Cl_2 from the alumina column, and the solvent was then removed. The resulting mixture was redissolved in a minimum amount of a 50/50 mixture of hexane/toluene and chromatographed on a SiO_2 column. Five bands were eluted from this second column: (1) the brown $Co_3Cp^*_2Cp'(\mu_3\text{-}CO)(\mu_3\text{-}NSiMe_3)$ (**2a**; 33 mg, 1%); (2) the brown-green $Co_3Cp^*Cp'_2(\mu_3\text{-}CO)(\mu_3\text{-}NSiMe_3)$ (**3a**; 135 mg, 3%); (3) the brown $Co_3Cp^*_2Cp'(\mu_3\text{-}CO)(\mu_3\text{-}NH)$ (**2**; 78 mg, 2%); (4) the brown-green $Co_3Cp'_3(\mu_3\text{-}CO)(\mu_3\text{-}NSiMe_3)$ (160 mg, 4%); and (5) the green $Co_3Cp^*Cp'_2(\mu_3\text{-}CO)(\mu_3\text{-}NH)$ (**3**; 140 mg, 3%).

2a was identified and characterized from spectral data. An IR spectrum (KBr pellet) of **2a** showed a triply bridging carbonyl stretching mode at 1660 cm^{-1}. A ^1H NMR spectrum ($CDCl_3$) exhibited an AA′BB′ pattern at δ 3.92 (m, 2 H) and δ 4.34 (m, 2 H) for the Cp′ ring protons, and at δ 2.03 (s, 3 H) for the corresponding methyl group. Methyl proton resonances for the two Cp* rings were observed at δ 1.57 (s, 30 H), while the silyl methyl hydrogen resonances were split into two singlets at δ 0.87 (s, 3 H) and δ 0.85 (s, 6 H).

3a was also characterized from spectral data. An IR spectrum (KBr pellet) contained an absorption band at 1660 cm^{-1} due to the triply bridging carbonyl. A ^1H NMR spectrum ($CDCl_3$) showed resonances for two different types of Cp′ ring hydrogens—viz., a single multiplet at δ 4.16 (m, 4 H) and an AA′BB′ pattern at δ 4.21 (m, 2 H) and δ 4.38 (m, 2 H). Resonances for the methyl groups from both Cp′ rings were observed at δ 1.92 (s, 6 H). The methyl hydrogens from the Cp* ring exhibited a resonance at δ 1.65 (s, 15 H), and those from the $NSiMe_3$ ligand at δ 0.83 (s, 9 H).

$Co_3Cp^*_2Cp'(\mu_3\text{-}CO)(\mu_3\text{-}NH)$ (**2**) was also characterized from spectral data. An IR spectrum (KBr pellet) showed an absorption band at 1670 cm^{-1} due to the triply bridging carbonyl. A ^1H NMR spectrum ($CDCl_3$) exhibited an AA′BB′ pattern at δ 3.96 (m, 2 H) and δ 4.34 (m, 2 H) for the Cp′ ring hydrogens and a singlet at δ 2.03 (s, 3 H) for the methyl hydrogens. The Cp* rings displayed a resonance at δ 1.64 (s, 30 H). A broad resonance centered at δ 12.09 was attributed to the NH hydrogen.

$Co_3Cp'_3(\mu_3\text{-}CO)(\mu_3\text{-}NSiMe_3)$ is a known compound that has been described elsewhere.[8]

$Co_3Cp^*Cp'_2(\mu_3\text{-}CO)(\mu_3\text{-}NH)$ (**3**) was characterized by spectral methods as well as by a single-crystal X-ray diffraction study. An IR spectrum (KBr pellet) displayed a strong triply bridging carbonyl stretch

(3) (a) Olson, W. L.; Schugart, K. A.; Fenske, R. F.; Dahl, L. F. In *Abstracts of Papers*, 187th National Meeting of the American Chemical Society, St. Louis, MO, American Chemical Society: Washington, DC, 1984; INOR 279. (b) Olson, W. L.; Dahl, L. F. *J. Am. Chem. Soc.* **1986**, *108*, 7657–7663.
(4) Olson, W. L.; Stacy, A. M.; Dahl, L. F. *J. Am. Chem. Soc.* **1986**, *108*, 7646–7656.
(5) Bray, A. C.; Green, M.; Hankey, D. R.; Howard, J. A. K.; Johnson, O.; Stone, F. G. A. *J. Organomet. Chem.* **1985**, *281*, C12–C16.
(6) Barnes, C. E.; Orvis, J. A.; Staley, D. L.; Rheingold, A. L.; Johnson, D. C. *J. Am. Chem. Soc.* **1989**, *111*, 4992–4994.
(7) Green, M.; Hankey, D. R.; Howard, J. A. K.; Louca, P.; Stone, F. G. A. *J. Chem. Soc. Chem. Commun.* **1983**, 757–758.
(8) Bedard, R. L.; Rae, D. A.; Dahl, L. F. *J. Am. Chem. Soc.* **1986**, *108*, 5924–5932.
(9) Bedard, R. L.; Dahl, L. F. *J. Am. Chem. Soc.* **1986**, *108*, 5933–5942.
(10) Pinhas, A. R.; Albright, T. A.; Hofmann, P.; Hoffmann, R. *Helv. Chim. Acta* **1980**, *63*, 29–49.
(11) Schilling, B. E. R.; Hoffmann, R. *J. Am. Chem. Soc.* **1979**, *101*, 3456–3467.
(12) Rives, A. B.; You, X.-Z.; Fenske, R. F. *Inorg. Chem.* **1982**, *21*, 2286–2294.
(13) Preliminary MO calculations[14] carried out on the 48-electron $Co_3Cp_3(\mu_3\text{-}CO)(\mu_3\text{-}NH)$ via the parameter-free Fenske–Hall method[15] revealed the HOMOs to be doubly degenerate (of e representation under C_{3v} symmetry). A comparative theoretical analysis of the 48-electron **1**, **2**, **3** and their $\mathbf{1}^+$, $\mathbf{2}^+$, $\mathbf{3}^+$ monocations is in progress.
(14) Spencer, B.; Ziebarth, M. S.; Shumaker, R. S.; Warta, C. L.; Dahl, L. F., unpublished observations.
(15) Hall, M. B.; Fenske, R. F. *Inorg. Chem.* **1972**, *11*, 768–775.
(16) Wei, C. H.; Dahl, L. F. *Inorg. Chem.* **1967**, *6*, 1229–1236.
(17) Strouse, C. E.; Dahl, L. F. *J. Am. Chem. Soc.* **1971**, *93*, 6027–6031.
(18) Frisch, P. D.; Dahl, L. F. *J. Am. Chem. Soc.* **1972**, *94*, 5082–5084.
(19) Kamijo, N.; Watanabe, T. *Acta Crystallogr.* **1979**, *B35*, 2537–2542.
(20) Pulliam, C. R.; Englert, M. H.; Dahl, L. F. *Abstracts of Papers*, 190th National Meeting of the American Chemical Society; American Chemical Society: Washington, DC, 1985; INOR 387.
(21) Wakatsuki, Y.; Okada, T.; Yamazaki, H.; Guobao, C. *Inorg. Chem.* **1988**, *27*, 2958–2963.
(22) Bedard, R. L.; Dahl, L. F. *J. Am. Chem. Soc.* **1986**, *108*, 5942–5948.
(23) (a) Kubat-Martin, K. A.; Rae, D. A.; Dahl, L. F. *Organomet. Chem.* **1985**, *4*, 2221–2223. (b) Kubat-Martin, K. A. Ph.D. Thesis, University of Wisconsin—Madison, June 1986.
(24) Rausch, M. D.; Genetti, R. A. *J. Org. Chem.* **1970**, *35*, 3883–3897.
(25) Cirjak, L. M.; Ginsburg, R. E.; Dahl, L. F. *Inorg. Chem.* **1982**, *21*, 940–957.

Table I. Crystal and Data Collection Parameters for $[Co_3Cp^*_3(\mu_3\text{-}CO)(\mu_3\text{-}NH)]^+[PF_6]^-$ ($[1]^+[PF_6]^-$), $[Co_3Cp^*_2Cp'(\mu_3\text{-}CO)(\mu_3\text{-}NH)]^+[PF_6]^-$ ($[2]^+[PF_6]^-$), $Co_3Cp^*Cp'_2(\mu_3\text{-}CO)(\mu_3\text{-}NH)$ (**3**), and $[Co_3Cp^*Cp'_2(\mu_3\text{-}CO)(\mu_3\text{-}NH)]^+[PF_6]^-$ ($[3]^+[PF_6]^-$)

	$[1]^+[PF_6]^-$	$[2]^+[PF_6]^-$	[3]	$[3]^+[PF_6]^-$
		A. Crystal Parameters		
formula	$C_{31}H_{46}NOF_6PCo_3$	$C_{27}H_{38}NOF_6PCo_3$	$C_{23}H_{30}NOCo_3$	$C_{23}H_{30}NOF_6PCo_3$
formula weight	770.5	714.4	513.3	658.3
crystal system	monoclinic	monoclinic	orthorhombic	monoclinic
a, Å	10.256 (7)	9.959 (7)	17.163 (12)	9.096 (7)
b, Å	19.481 (9)	15.726 (10)	13.548 (7)	18.340 (14)
c, Å	16.557 (7)	18.697 (9)	9.131 (6)	15.212 (15)
α, deg	90	90	90	90
β, deg	90.85 (4)	91.66 (7)	90	96.44 (7)
γ, deg	90	90	90	90
V, Å^3	3308 (3)	2927 (3)	2131 (2)	2522 (4)
space group	$P2_1/c$	$P2_1/n$	$Pnma$	$P2_1/c$
Z	4	4	4	4
d(calcd), g/cm^3	1.55	1.62	1.58	1.58
μ(calcd), cm^{-1}	15.91	17.9	23.4	20.7
		B. Data Measurement Parameters		
data collect temp, °C	−100	−60	−80	−80
scan mode	Wyckoff ω	Wyckoff ω	Wyckoff ω	Wyckoff ω
scan speed, deg/min	variable (4–29.3)	variable (4–29.3)	variable (4–29.3)	variable (4–29.3)
2θ limits. deg	4–48	4–47	4–58	4–48
no. of check reflctns/freq	3/47	3/47	3/47	3/47
cuttoff for obsd data	$\|F\| > 4\sigma(F)$	$\|F\| > 4\sigma(F)$	$\|F\| > 6\sigma(F)$	$\|F\| > 3\sigma(F)$
no. of obsd reflctns	2486	2779	1812	2513
no. of refined param	304	321	148	331
data/parameter ratio	8.2:1	8.7:1	12.2:1	7.6:1
anisotropic conv, %	R_1 = 9.44; R_2 = 8.77	R_1 = 7.17; R_2 = 7.48	R_1 = 4.99; R_2 = 6.58	R_1 = 7.84; R_2 = 6.37
goodness of fit	1.67	1.75	1.40	1.39

at 1640 cm^{-1} and a weak, sharp N–H stretching band at 3200 cm^{-1}. A ^{1}H NMR spectrum ($CDCl_3$) exhibited a single multiplet at δ 4.31 (m, 4 H) for the ring hydrogens on one Cp′ ligand and an AA′BB′ pattern at δ 4.23 (m, 2 H) and δ 4.16 (m, 2 H) for the ring protons on the other Cp′ ligand. The two methyl groups from the Cp′ ligands displayed a resonance at δ 1.93 (s, 6 H), and the Cp* ring exhibited a resonance at δ 1.66 (s, 15 H). A broad 1:1:1 pattern centered at δ 12.86 was attributed to the NH hydrogen.

Preparation of the Mixed Cp*/Cp′ $Co_3Cp^*_{3-x}Cp'_x(\mu_3\text{-}CO)(\mu_3\text{-}NH)$ Clusters [x = 1 (2), 2 (3)] from Reactions of the Corresponding $Co_3Cp^*_{3-x}Cp'_x(\mu_3\text{-}CO)(\mu_3\text{-}NSiMe_3)$ Clusters [x = 1 (2a), 2 (3a)] with $[(n\text{-}Bu)_4N]^+[F]^-\cdot 3H_2O$. Stoichiometric amounts of $Co_3Cp^*_{3-x}Cp'_x(\mu_3\text{-}CO)(\mu_3\text{-}NSiMe_3)$ [where x = 1 (**2a**) or 2 (**3a**)] and $[(n\text{-}Bu)_4N]^+[F]^-\cdot 3H_2O$ were stirred at room temperature in CH_2Cl_2. After 2 h the solvent was removed under vacuum, and the product was extracted with toluene. With this procedure, yields of greater than 90% for the conversion of **2a** (x = 1) and **3a** (x = 2) to **2** and **3**, respectively, were obtained.

Preparation of the Oxidized 47-Electron $[Co_3Cp^*_{3-x}Cp'_x(\mu_3\text{-}CO)(\mu_3\text{-}NH)]^+$ Monocations [x = 0 (1^+); x = 1 (2^+); x = 2 (3^+)]. Equimolar quantities of **3** and $AgPF_6$ were stirred in 50 mL of CH_2Cl_2 at room temperature for 30 min. The color of the solution turned from brown to red over this time period. The solvent was then removed and the residue washed with toluene to remove any leftover starting material. The toluene-insoluble material was then extracted with CH_2Cl_2 to give $[Co_3Cp^*Cp'_2(\mu_3\text{-}CO)(\mu_3\text{-}NH)]^+$ (3^+) as the hexafluorophosphate salt. The $[PF_6]^-$ salts of 1^+ and 2^+ were prepared by similar procedures.

All three of these 47-electron tricobalt monocations were characterized from their IR spectra and single-crystal X-ray structural analyses. IR spectra (KBr pellet) of the three homologous $[Co_3Cp^*_{3-x}Cp'_x(\mu_3\text{-}CO)(\mu_3\text{-}NH)]^n$ pairs (n = 0, +1 for x = 0, 1, 2) exhibited the following shifts in the triply bridging carbonyl bands: 1635 cm^{-1} for **1** (n = 0) to 1720 cm^{-1} for 1^+ (n = +1); 1670 cm^{-1} for **2** (n = 0) to 1745 cm^{-1} for 2^+ (n = +1); 1640 cm^{-1} for **3** (n = 0) to 1748 cm^{-1} for 3^+ (n = +1). As expected for paramagnetic species, none of the 47-electron clusters exhibited a ^{1}H NMR spectrum.

EPR Spectra of $[Co_3Cp^*_3(\mu_3\text{-}CO)(\mu_3\text{-}NH)]^+$ (1^+) and $[Co_3Cp^*_2Cp'(\mu_3\text{-}CO)(\mu_3\text{-}NH)]^+$ (2^+). No EPR signals were observed for the $[PF_6]^-$ salts of 1^+ and 2^+ either in solutions at room temperature or in frozen glass at low temperature (100 K).

X-ray Structural Determination of $[Co_3Cp^*_3(\mu_3\text{-}CO)(\mu_3\text{-}NH)]^+[PF_6]^-$. Diffraction-quality crystals were produced when diisopropyl ether was allowed to diffuse slowly into a concentrated solution of the $[PF_6]^-$ salt of 1^+ in methylene chloride. A parallelepiped-shaped crystal of dimensions 0.6 × 0.2 × 0.2 mm was mounted inside an argon-filled Lindemann glass capillary, which was then hermetically sealed. A Nicolet P3/F diffractometer with Mo Kα radiation was utilized for data collection at −100 °C. Axial photographs taken about the three principal axes indicated a monoclinic cell. Specific details of this structure are listed in Table I.

Systematic absences uniquely define the probable space group as $P2_1/c$. One 1^+ monocation and one hexafluorophosphate counterion comprise the crystallographically independent unit. The structure was solved and refined with the SHELXTL Plus package.[26] The positions of the cobalt atoms in the cell were found by direct methods, and the other non-hydrogen atoms were determined by successive Fourier difference maps. The ring carbon atoms for each of the three Cp* ligands were constrained to 5-fold symmetry with bond lengths fixed at 1.42 Å, but the methyl carbon atoms were allowed to refine without any constraints. All three of the pentamethylcyclopentadienyl ligands were rotationally disordered between two staggered positions with the following least-squares refined occupancies: ring 1 (57/43), ring 2 (60/40), and ring 3 (51/49). The six fluorine atoms in the hexafluorophosphate counterion were also disordered into two distinct octahedral arrangements of fluorine atoms around the center phosphorus atom with refined site occupancies of 63% and 37%. All hydrogen atoms, except the imido hydrogen atom whose position was located from a Fourier difference map, were fixed at idealized positions and refined with isotropic thermal parameters set at U = 0.06 Å^2. Due to the crystal disorder of the pentamethylcyclopentadienyl rings and the hexafluorophosphate counterion, only the non-hydrogen atoms of the $Co_3(\mu_3\text{-}CO)(\mu_3\text{-}NH)$ core were refined anisotropically. An empirical absorption correction was applied to the data.[27] Refinement converged at $R_1(F)$ = 9.44, $R_2(F)$ = 8.77 with a goodness-of-fit value of 1.67. The data-to-parameter ratio was 8.2/1 for 2486 independent reflections with $|F| > 4\sigma(F)$. A final electron-density map revealed no unusual features. Tables of positional parameters and equivalent isotropic thermal parameters, anisotropic thermal parameters, interatomic distances, bond angles, parameters for hydrogen atoms, and a listing of observed and calculated structure factor amplitudes are available as supplementary material.

X-ray Structural Determination of $[Co_3Cp^*_2Cp'(\mu_3\text{-}CO)(\mu_3\text{-}NH)]^+[PF_6]^-$. Diffraction-quality crystals were obtained by the slow diffusion of diisopropyl ether into a concentrated solution of the $[PF_6]^-$ salt of 2^+ in methylene chloride. A dark red parallelepiped-shaped crystal of dimensions 1.0 × 0.2 × 0.2 mm was hermetically sealed inside an argon-filled Lindemann glass capillary. Intensity data were collected on a Nicolet P3/F diffractometer with Mo Kα radiation at −60 °C. Axial photographs confirmed the symmetry of the cell and the approximate

(26) (a) Sheldrick, G. M.; Schenk, H.; Olthof-Hazekamp, R.; Van Koningsveld, H.; Bassi, G. C. *Computing in Crystallography*; Delft University Press: Delft, The Netherlands, 1978. (b) Users Guide for SHELXTL, Nicolet Analytical Instruments, Madison, WI, 1986.

(27) Empirical corrections based on ψ-scan measurements at different azimuthal angles were calculated with the XEMP program (SHELXTL).

axial lengths. Crystal data and data collection parameters are given in Table I.

The probable space group $P2_1/n$ was uniquely indicated by the systematic absences. The SHELXTL Plus package[26] was used to solve and refine the structure. Heavy-atom positions were determined by direct methods, and the other non-hydrogen atoms were located by successive Fourier difference maps. One of the pentamethylcyclopentadienyl rings was rotationally disordered between staggered orientations. The ring carbon atoms in each of the orientations were constrained to D_{5h} symmetry with a fixed C–C bond distance of 1.42 Å. The site occupancy factor refined to 54% for one ring and 46% for the other. The other pentamethylcyclopentadienyl and methylcyclopentadienyl ligands as well as all the methyl groups in the Cp* group were refined without constraints. The fluorine atoms in the hexafluorophosphate anion were also disordered into two different octahedral arrangements of fluorine atoms around the center phosphorus atom with refined site occupancies of 64% and 36%. All hydrogen atoms were fixed at idealized positions with isotropic thermal parameters of $U = 0.06$ Å^2. All non-hydrogen atoms, except those in the disordered parts of the molecule, were refined anisotropically. An empirical absorption correction was applied to the data.[27] Structure refinement converged at $R_1(F) = 7.17$, $R_2(F) = 7.48$ with a goodness of fit of 1.75. The final data-to-parameter ratio was 8.7/1 for 2779 reflections with $|F| > 4\sigma(F)$. A final electron-density difference map showed no abnormal residual electron density. Tables of the atomic parameters for the non-hydrogen atoms, anisotropic thermal parameters, interatomic distances, bond angles, hydrogen atomic parameters, and a listing of observed and calculated structure factor amplitudes are available as supplementary material.

X-ray Structural Determination of $Co_3Cp^*Cp'_2(\mu_3\text{-}CO)(\mu_3\text{-}NH)$ (3). Crystals of diffraction quality were obtained by allowing a concentrated hexane/methylene chloride solution of **3** to slowly evaporate. A dark parallelepiped-shaped crystal of dimensions 0.80 × 0.27 × 0.45 mm was inserted under argon into a Lindemann glass capillary, which was then hermetically sealed. Intensity data were collected on a Nicolet P3/F diffractometer with Mo Kα radiation at −80 °C. Axial photographs about the principal axes indicated that the cell was orthorhombic. Specific details concerning crystal data collection are listed in Table I.

Systematic absences indicated two probable space groups, either the centrosymmetric *Pnma* or the noncentrosymmetric $Pn2_1a$ (nonstandard setting of $Pna2_1$). A statistical analysis of the data indicated that the space group was centrosymmetric, and the successful solution under *Pnma* corroborated this choice. This space group imposes crystallographic C_s-*m* site symmetry on each molecule with $Z = 4$. The SHELXTL Plus package[26] was used to solve and refine the structure. Direct methods were used to find the heavy-atom positions, and the other non-hydrogen atoms were located through subsequent Fourier difference maps. The imido hydrogen atom was located from a Fourier difference map, while all other hydrogen atoms were fixed at idealized positions and refined with isotropic thermal parameters set at $U = 0.06$ Å^2. An empirical absorption correction based on ψ-scans was applied to the data.[27] Anisotropic refinement of all non-hydrogen atoms gave $R_1(F) = 4.99$, $R_2(F) = 6.58$ with a goodness of fit of 1.398. The final data-to-parameter ratio for 1812 independent reflections with $|F| > 6\sigma(F)$ was 12.2/1. A final Fourier difference map showed no residual electron-density peaks greater than 1.0 e ln/Å^3. Tables of parameters for the non-hydrogen atoms, anisotropic thermal parameters, appropriate interatomic distances, bond angles, parameters for the hydrogen atoms, and a listing of observed and calculated structure factor amplitudes are available as supplementary material.

X-ray Structural Determination of $[Co_3Cp^*Cp'_2(\mu_3\text{-}CO)(\mu_3\text{-}NH)]^+[PF_6]^-$. Crystals of diffraction quality were obtained by a careful layering of diisopropyl ether on a concentrated solution of the $[PF_6]^-$ salt of $\mathbf{3}^+$ in CH_2Cl_2. A parallelepiped-shaped crystal of 1.0 × 0.15 × 0.15 mm dimensions was mounted under argon in a Lindemann glass capillary, which was then hermetically sealed. Intensity data were collected at −80 °C on a Nicolet P3/F diffractometer with Mo Kα radiation. Axial photographs about the principal axes gave approximate lattice parameters and indicated monoclinic symmetry. Crystal and data collection parameters are given in Table I.

Observed systematic absences uniquely define the space group as $P2_1/c$. The solution and refinement of the crystal structure were carried out via the SHELXTL Plus package.[26] Direct methods were used to determine the heavy-atom positions, and the other non-hydrogen atoms were located from subsequent Fourier difference maps. Hydrogen atoms were fixed in idealized positions with bond lengths of 0.96 Å and isotropic thermal parameters of $U = 0.06$ Å^2. The hexafluorophosphate counterion was disordered and modeled into three orientations. The data were corrected for absorption by the ψ-scan method.[27] Least-squares refinement with anisotropic thermal parameters utilized for all nondisordered, non-hydrogen atoms converged at $R_1(F) = 7.84$, $R_2(F) = 6.37$ with a goodness of fit of 1.39. The final data-to-parameter ratio was 7.6/1 for 2513 independent reflections with $|F| > 3\sigma(F)$. Tables containing parameters for the nonhydrogen atoms, anisotropic thermal parameters, interatomic distances, bond angles, parameters for the hydrogen atoms, and a listing of observed and calculated structure factor amplitudes are available as supplementary material.

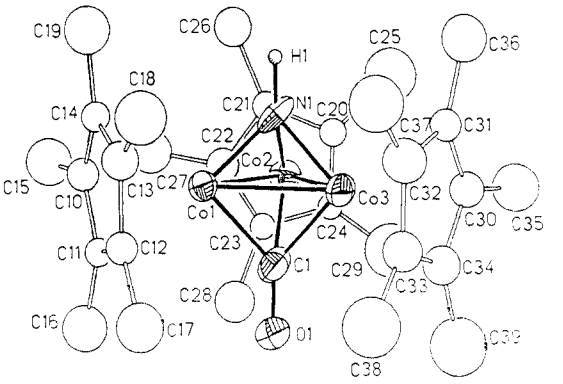

Figure 1. View of the 47-electron $[Co_3Cp^*_3(\mu_3\text{-}CO)(\mu_3\text{-}NH)]^+$ monocation ($\mathbf{1}^+$), which has no crystallographically imposed symmetry. Only one orientation for each of the crystal-disordered C_5Me_5 rings is shown. The position of the nitrene hydrogen atom was located from an electron-density difference synthesis. No discernible geometrical distortion of the $Co_3(CO)(NH)$ core from pseudo-C_{3v}-$3m$ symmetry is observed.

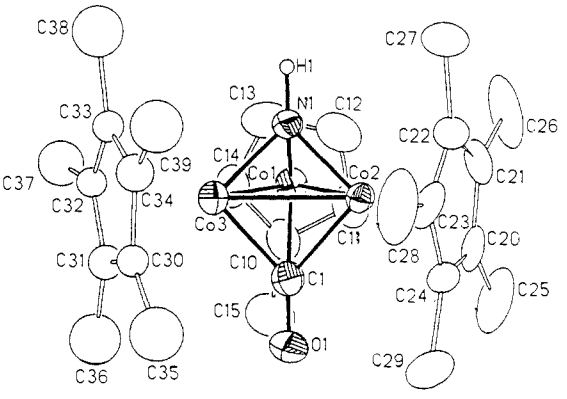

Figure 2. View of the 47-electron $[Co_3Cp^*_2Cp'(\mu_3\text{-}CO)(\mu_3\text{-}NH)]^+$ monocation ($\mathbf{2}^+$), which has no crystallographically imposed symmetry. Only one orientation of the crystal-disordered Cp* ring attached to Co(3) is shown. The geometry of the $Co_3(CO)(NH)$ core of $\mathbf{2}^+$, which has one Cp′ and two Cp* ligands, is markedly distorted from pseudo-C_{3v}-$3m$ to pseudo-C_s-*m* symmetry.

Results and Discussion

Structural Features. (a) $[Co_3Cp^*_3(\mu_3\text{-}CO)(\mu_3\text{-}NH)]^+[PF_6]^-$. The $[PF_6]^-$ salt of $\mathbf{1}^+$ exists in the solid state as discrete cations and anions and has no unusual interionic contacts. The hexafluorophosphate anion is disordered into two distinct octahedral orientations with occupancy factors of 63% and 37%.

The solid-state configuration of the $Co_3(CO)(NH)$ core of $\mathbf{1}^+$ approximately conforms to C_{3v} geometry. Each of the three Cp* ligands in $\mathbf{1}^+$ has a rotational crystal disorder involving an essentially random occupancy of one of two staggered orientations. Only one of the orientations is shown for each of the Cp* ligands in Figure 1. Despite the disorder of the Cp* ligands, the atomic thermal ellipsoids appear to be normal for the $Co_3(CO)(NH)$ core.

(b) $[Co_3Cp^*_2Cp'(\mu_3\text{-}CO)(\mu_3\text{-}NH)]^+[PF_6]^-$. The crystal packing of the $\mathbf{2}^+$ monocations and $[PF_6]^-$ monoanions in this crystal structure appears to be normal with no unusual interionic contacts. The independent hexafluorophosphate anion, which is disordered into two distinct orientations with site occupancies of 64% and 36%, exhibits normal distances and bond angles.

The overall configuration of the independent $\mathbf{2}^+$ monocation conforms closely to C_s-*m* geometry except for the Cp′ methyl carbon atom, which is rotated by ca. 10° off the pseudomirror plane. One of the Cp* ligands has a rotational crystal disorder with occupancy factors for the two staggered orientations of 54%

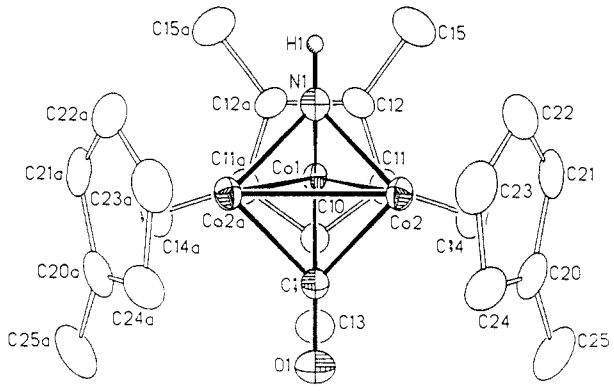

Figure 3. A view of the 48-electron $Co_3Cp^*Cp'_2(\mu_3\text{-}CO)(\mu_3\text{-}NH)$ (**3**), which has crystallographic C_s-m site symmetry. The position of the nitrene hydrogen atom was located from a Fourier difference map. The geometry of the $Co_3(CO)(NH)$ core closely approximates C_{3v}-$3m$ symmetry.

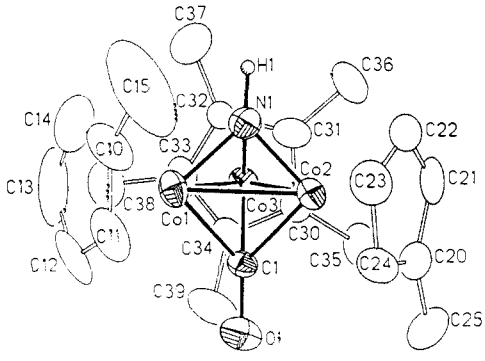

Figure 4. View of the 47-electron $[Co_3Cp^*Cp'_2(\mu_3\text{-}CO)(\mu_3\text{-}NH)]^+$ monocation (3^+), which has no crystallographically imposed symmetry. The geometry of the $Co_3(CO)(NH)$ core of 3^+, which has one Cp* and two Cp′ ligands, is markedly distorted from pseudo-C_{3v}-$3m$ symmetry to pseudo-C_s-m symmetry.

and 46%; only one of its positions is shown in Figure 2. The geometry of the $Co_3(CO)(NH)$ core also conforms to pseudo-C_s-m symmetry with the mirror plane bisecting the long Co–Co bond and mirror-relating the two shorter Co–Co bonds.

(c) $Co_3Cp^*Cp'_2(\mu_3\text{-}CO)(\mu_3\text{-}NH)$ (3). The crystal structure of **3** has crystallographically imposed C_s-m site symmetry, with the mirror passing through Co(1) and the two capping ligands and bisecting the Co(2)–Co(3) bond and the Cp* ligand (Figure 3). The $Co_3(CO)(NH)$ core closely conforms to pseudo-C_{3v} symmetry.

An interesting packing feature in this crystal structure is the hydrogen-bonding interaction of the capping imido hydrogen atom with the capping carbonyl oxygen atom. This NH···O interaction, which gives rise to observed N···O and H···O distances of 3.03 and 2.2 Å, respectively, causes a stacking of the molecules into linear chains in the solid state. No other unusual intermolecular interactions are observed.

(d) $[Co_3Cp^*Cp'_2(\mu_3\text{-}CO)(\mu_3\text{-}NH)]^+[PF_6]^-$. The 3^+ monocations and $[PF_6]^-$ monoanions are well separated in this crystal structure with no unusual packing interactions. The independent hexafluorophosphate counterion has a 30°-related rotational crystal disorder of the four perpendicular fluorine atoms around one trans F–P–F axis with three orientations for these four fluorine atoms of 54%, 26%, and 20% site occupancies.

The 3^+ monocation has an idealized C_s-m geometry except for the two mirrored Cp′ ligands whose methyl groups are rotated by ca. 180° to each other (Figure 4). The $Co_3(CO)(NH)$ core corresponds closely to C_s-m symmetry, with one shorter and two longer Co–Co bonds and one short Co–CO bond distorting it from an idealized C_{3v} geometry possessed by its neutral parent.

Comparative Analysis of the Geometries of the 48-Electron $Co_3Cp^*_3(\mu_3\text{-}CO)(\mu_3\text{-}NH)$ (1) with the 47-Electron $[Co_3Cp^*_3(\mu_3\text{-}CO)(\mu_3\text{-}NH)]^+$ Monocation (1^+). An examination of Table II reveals the structural changes associated with the oxidation of

Table II. Comparison of Distances and Bond Angles for the 48-Electron $Co_3Cp^*_3(\mu_3\text{-}CO)(\mu_3\text{-}NH)$ (**1**)[a] of Crystallographic C_s-m Site Symmetry and Its 47-Electron $[Co_3Cp^*_3(\mu_3\text{-}CO)(\mu_3\text{-}NH)]^+$ Monocation (1^+)[b] of Crystallographic C_1-1 Site Symmetry

	1	1^+
A. Distances, Å		
Cp*Co-CoCp*	2.419 (4)	2.401 (3)
	2.432 (3)	2.404 (3)
	2.432 (3)	2.423 (3)
mean Cp*Co–CoCp*	2.428[c]	2.409[c]
Cp*Co–NH	1.825 (14)	1.799 (12)
	1.837 (13)	1.815 (12)
	1.837 (13)	1.829 (12)
mean Cp*Co–NH	1.833[c]	1.814[c]
Cp*Co–CO	1.921 (22)	1.975 (17)
	1.935 (16)	1.968 (16)
	1.935 (16)	1.995 (17)
mean Cp*Co–CO	1.930[c]	1.979[c]
C–O	1.232 (21)	1.192 (20)
mean Co-Cp*(c)[d]	1.72[c]	1.71[c]
B. Bond Angles, deg		
Cp*Co–C(O)–CoCp*	77.4 (6)	75.8 (6)
	78.2 (8)	74.5 (6)
	78.2 (8)	74.6 (6)
mean Cp*Co–C(O)–CoCp*	77.9[c]	75.0[c]
Cp*Co–N(H)–CoCp*	82.3 (5)	84.2 (6)
	83.2 (6)	83.0 (5)
	83.2 (6)	82.4 (5)
mean Cp*Co–N(H)–CoCp*	82.9[c]	83.2[c]

[a] Reference 8. [b] $[PF_6]^-$ salt. [c] Means are calculated under assumed C_{3v}-$3m$ symmetry. [d] Cp*(c) denotes the centroid of the C_5Me_5 ring.

1 to 1^+. The tricobalt core of C_s-m site symmetry in **1** approximates an equilateral triangle; the two identical Co–Co bond lengths of 2.432 (3) Å and the third Co–Co bond length of 2.419 (4) Å are within 0.01 Å of the mean bond length of 2.428 Å.[8] The tricobalt core in the 47-electron 1^+ is also only slightly distorted from an equilateral cobalt triangle with sides of 2.423 (3), 2.401 (3), and 2.404 (3) Å and a mean of 2.409 Å. The 0.019-Å shortening in the mean Co–Co distance obtained upon removal of an electron from the filled degenerate e HOMOs (under assumed C_{3v} symmetry) is consistent with the HOMOs containing relatively little tricobalt *antibonding* character. The absence of any discernible Jahn–Teller deformation of the metal framework in the monocation (1^+) may be rationalized on the basis that the doubly degenerate e HOMOs. which are filled in the 48-electron **1** and $^3/_4$ filled in the 47-electron 1^+ under C_{3v} symmetry, lack appreciable tricobalt antibonding character. The prediction of considerable trimetal antibonding character, based on the MO correlation diagram presented by Hoffmann and co-workers[10] for the hypothetical 46-electron $Rh_3Cp_3(\mu_3\text{-}CO)_2$ under D_{3h} symmetry, may not be valid in the case of **1** and 1^+ due to extensive mixing of the in-plane trimetal bonding and the out-of-plane trimetal antibonding MOs under the lower C_{3v} symmetry.

The changes in the mean distances between the cobalt atoms and the capping CO and NH ligands associated with the oxidation of **1** to 1^+ reflect the loss of electron density from the trimetal cluster. A significant decrease in back-bonding from the metal orbitals to the π^*-acceptor carbonyl orbitals in 1^+ is evidenced by the 0.05-Å increase in the mean Co–CO distance. However, all three Co–CO bond lengths of 1.968 (16), 1.975 (17), and 1.995 (17) Å in 1^+ are equivalent within experimental error. In the case of the π-donor (nonhybridized) nitrene ligand, the mean of the two independent, experimentally equivalent Cp*Co–NH bond lengths in **1** is 1.833 Å, while the mean of the three experimentally equivalent Cp*Co–NH bond lengths in 1^+ is 1.814 Å. The 0.02-Å decrease in the mean Cp*Co–NH bond upon oxidation of **1** to 1^+ indicates that the NH ligand is a better electron donor in the monocation. The absence of any pronounced variations in the individual Cp*Co–CO and/or Cp*Co–NH bonds in 1^+ suggests that the Jahn–Teller distortion either is distributed over the entire monocation instead of being concentrated in a particular part of the $Co_3(CO)(NH)$ core or is mainly a consequence of instantaneous deformations of the Cp* ligands from the non-3-fold mo-

Table III. Distances and Bond Angles for the 47-Electron $[Co_3Cp^*_2Cp'(\mu_3\text{-}CO)(\mu_3\text{-}NH)]^+$ Monocation (2^+)[a] of Crystallographic C_1-1 Site Symmetry

A. Distances, Å			
Cp*Co–CoCp′	2.359 (2)	Cp′Co–CO	2.099 (12)
Cp*Co–CoCp′	2.367 (2)	Cp*Co–CO	1.951 (11)
Cp*Co–CoCp*	2.443 (2)	Cp*Co–CO	1.942 (11)
mean Co–Co′	2.390[b]	mean Co–CO	1.997[b]
Cp′Co–NH	1.820 (8)	C–O	1.232 (21)
Cp*Co–NH	1.808 (8)	mean Co–Cp*(c)[c]	1.69
Cp*Co–NH	1.809 (8)	Co–Cp′(c)[c]	1.71
mean Co–NH	1.812[b]		
B. Bond Angles, deg			
Cp*Co–C(O)–CoCp′	71.1 (4)	Cp*Co–N(H)–CoCp′	81.3 (3)
Cp*Co–C(O)–CoCp′	71.6 (4)	Cp*Co–N(H)–CoCp′	81.4 (3)
Cp*Co–C(O)–CoCp*	77.7 (4)	Cp*Co–N(H)–CoCp*	85.0 (3)
mean Co–C(O)–Co	73.5[b]	mean Co–N(H)–Co	82.6[b]

[a] $[PF_6]^-$ salt. [b] Means are calculated under assumed C_{3v}-3m symmetry. [c] Cp*(c) and Cp′(c) denote the centroids of the C_5Me_5 and C_4H_4Me rings, respectively.

lecular symmetry splitting the degeneracy of the $^3/_4$-filled HOMOs. A third distinct possibility is that the $Co_3(CO)(NH)$ core of 1^+ is 3-fold disordered in the solid state even though the crystallographic site symmetry is C_1-1.

Analysis of the Geometry of the 47-Electron $[Co_3Cp^*_2Cp'(\mu_3\text{-}CO)(\mu_3\text{-}NH)]^+$ Monocation (2^+). Table III presents the salient bond distances and angles for the 2^+ monocation. The geometry of the $Co_3(CO)(NH)$ core of 2^+, which contains one Cp′ and two Cp* ligands, is markedly distorted from pseudo-C_{3v}-3m to pseudo-C_s-m symmetry. The Cp*Co-CoCp* bond of 2.443 (2) Å is 0.08 Å longer than the two Cp*Co–CoCp′ bonds of 2.359 (2) and 2.367 (2) Å, while the two Cp*Co–CO distances of 1.94 (1) and 1.95 (1) Å are 0.15 Å shorter than the Cp′Co–CO distance of 2.10 (1) Å. On the other hand, the Cp′Co–NH bond of 1.820 (8) Å is not significantly longer than the two Cp*Co–NH bonds of 1.808 (8) and 1.809 (8) Å. This preferential elongation of the Cp′Co–CO bond is attributed to the less electron-releasing terminal Cp′ ligand producing a smaller electron density on its attached Co atom which, in turn, results in smaller π back-bonding to the capping carbonyl. This large distortion toward a semibridging carbonyl in 2^+ indicates that its $^3/_4$-filled HOMOs are composed of a large percentage of back-bonding $d\pi(Co)$–$\pi^*(CO)$ orbital character, which mainly involves the higher energy Cp*Co fragments.

Comparative Analysis of the Geometries of the 48-Electron $Co_3Cp^*Cp'_2(\mu_3\text{-}CO)(\mu_3\text{-}NH)$ (3) with the 47-Electron $[Co_3Cp^*Cp'_2(\mu_3\text{-}CO)(\mu_3\text{-}NH)]^+$ Monocation (3^+). Table IV shows the distances and bond angles for **3** and 3^+. Oxidation of **3**, which has one Cp* and two Cp′ ligands and conforms to mirror plane symmetry, to 3^+ also produces a discernible geometrical deformation of the $Co_3(CO)(NH)$ core from pseudo-C_{3v} symmetry to pseudo-C_s symmetry. The two mirror-related Cp*Co–CoCp′ bonds of 2.395 (1) Å in **3** are slightly increased to 2.407 (2) and 2.409 (2) Å in 3^+, while the Cp′Co–CoCp′ bond of 2.375 (1) Å in **3** is decreased to 2.350 (2) Å in 3^+. The mean Co–Co distance of 2.388 Å in **3** is virtually identical with that of 2.389 Å in 3^+. The Cp*Co–CO bond distance in **3** is 0.02 Å shorter than the two mirror-related Cp′Co–CO bond lengths, but in 3^+ this difference is increased to 0.07 Å. The mean of 1.814 Å for the virtually identical Cp*Co–NH and Cp′Co–NH bond lengths in **3** is shortened to 1.787 Å for the experimentally equivalent Cp*Co–NH and Cp′Co–NH bond lengths in 3^+.

Small decreases in the Co–Cp* (centroid) and Co–Cp′(centroid) distances of 0.01 and 0.02 Å, respectively, also occur upon oxidation of **3** to 3^+. These small variations are consistent with that found for the Co–Cp* (centroid) distances upon oxidation of **1** to 1^+.

Influence of Cp* versus Cp′ Ligands on the Geometries of the 48/47-Electron Triangular Metal Clusters, $[Co_3Cp^*_{3-x}Cp'_x(\mu_3\text{-}CO)(\mu_3\text{-}NH)]^n$ (x = 0, n = 0, +1; x = 1, n = +1; x = 2, n = 0, +1). The influence of the terminal Cp* and Cp′ ligands on the capping ligand in **1**, 1^+, 2^+, **3**, and 3^+ is negligible in the case of the capping nitrene ligand and substantial in the case of the capping carbonyl ligand. The Cp*Co–NH and Cp′Co–NH distances within a given tricobalt cluster are experimentally equivalent. The decrease in the mean Co–NH distance by 0.019 Å upon oxidation of **1** to 1^+ and by 0.027 Å upon oxidation of **3** to 3^+ is ascribed to NH being a better electron donor in the oxidized 47-electron species. Tables II–IV show that the Co–N(H)–Co bond angles vary from 81.3 (3) to 85.0 (3)°. The distribution of this small angular range of 3.7° is *not* dependent on whether the cobalt atoms are attached to Cp* or Cp′.

Table IV. Comparison of Distances and Bond Angles for the 48-Electron $Co_3Cp^*Cp'_2(\mu_3\text{-}CO)(\mu_3\text{-}NH)$ (**3**) of Crystallographic C_s-m Site Symmetry and Its 47-Electron $[Co_3Cp^*Cp'_2(\mu_3\text{-}CO)(\mu_3\text{-}NH)]^+$ Monocation (3^+)[a] of Crystallographic C_1-1 Site Symmetry

	3	3^+
A. Distances, Å		
Cp*Co–CoCp′	2.395 (1)	2.409 (2)
Cp*Co–CoCp′	2.395 (1)	2.407 (2)
Cp′Co–CoCp′	2.375 (1)	2.350 (2)
mean Co–Co′	2.388[b]	2.389[b]
Cp*Co–NH	1.812 (7)	1.793 (8)
Cp′Co–NH	1.815 (5)	1.785 (9)
Cp′Co–NH	1.815 (5)	1.782 (8)
mean Co–NH	1.814[b]	1.787[b]
Cp*Co–CO	1.935 (7)	1.875 (10)
Cp′Co–CO	1.957 (6)	1.926 (9)
Cp′Co–CO	1.957 (6)	1.964 (10)
mean Co–CO	1.950[b]	1.922[b]
C–O	1.200 (9)	1.208 (12)
Co–Cp*(c)[c]	1.67	1.66
mean Co–Cp′(c)[c]	1.70	1.68
B. Bond Angles, deg		
Cp′Co–C(O)–CoCp*	76.0 (2)	77.6 (4)
Cp′Co–C(O)–CoCp*	76.0 (2)	78.6 (4)
Cp′Co–C(O)–CoCp′	74.7 (3)	74.3 (3)
mean Co–C(O)–Co	75.6[b]	76.8[b]
Cp′Co–N(H)–CoCp*	82.7 (3)	84.7 (3)
Cp′Co–N(H)–CoCp*	82.7 (3)	84.6 (4)
Cp′Co–N(H)–CoCp′	81.7 (3)	82.4 (4)
mean Co–N(H)–Co	82.4[b]	83.9[b]

[a] $[PF_6]^-$ salt. [b] Means are calculated under assumed C_{3v}-3m symmetry. [c] Cp*(c) and Cp′(c) denote the centroids of the C_5Me_5 and C_4H_4Me rings, respectively.

In contrast, the replacement of a Cp* ligand with a Cp′ ligand has a large effect on the capping carbonyl in these tricobalt clusters. Since the triply bridging carbonyl is a π-acceptor ligand, it will form stronger, shorter bonds to metals with more electron density for π back-bonding. The bond-length variations stress that the metal–metal distances in the $Co_3(CO)(NH)$ cores of these 47/48-electron clusters are strongly influenced by the Cp*Co–CO and Cp′Co–CO distances with the former being invariably smaller within a given mixed Cp*/Cp′ cluster due to greater π back-bonding from the higher energy CoCp* $d\pi$ AOs to the empty CO π^*-acceptor orbitals. This shortening of the Cp*Co–CO distance relative to the Cp′Co–CO distance in the 48-electron **3** is 0.022 Å. In the 47-electron systems this effect is magnified, the difference in the shorter Cp*Co–CO distance relative to the Cp′Co–CO distance in 2^+ being 0.15 Å and in 3^+ being 0.07 Å.

The individual Co–C(O)–Co bond angles in **1**, 1^+, 2^+, **3**, and 3^+ vary from 71.1 (4)° in 2^+ to 78.6 (4)° in 3^+. Most of the larger angles are associated with two CoCp* fragments. The decrease in the mean Cp*Co–C(O)–CoCp* bond angle from 77.9° in **1** to 75.0° in 1^+ is inversely correlated with the increase in mean Cp*Co–CO distance from 1.930 Å in **1** to 1.979 Å in 1^+. This 2.9° smaller Cp*Co–C(O)–CoCp* bond angle with a 0.049-Å longer Cp*Co–CO distance in 1^+ results in the mean Cp*Co–CoCp* bond length in 1^+ being only 0.019 Å shorter than that in **1**. In 2^+ the two 0.15-Å shorter Cp*Co–CO distances of 1.946 Å (av) are associated with a 0.08-Å longer Cp*Co–CoCp* distance of 2.443 (2) Å due to a 6.3° wider Cp*Co–C(O)–CoCp* bond angle of 77.7 (4)°. In the C_s-m **3**, the one 0.022-Å shorter Cp*Co–CO distance of 1.935 (7) Å is associated with two 0.02-Å

longer Cp*Co–CoCp′ distances of 2.395 (1) Å due to the two identical 1.3° wider Cp*Co–C(O)–CoCp′ bond angles of 76.0 (2)°. In 3^+, the one 0.07-Å shorter Cp*Co–CO distance is associated with two 0.06-Å longer Cp*Co–CoCp′ distances of 2.408 Å (av) due to two 3.8° wider Cp*Co–C(O)–CoCp′ bond angles of 78.1° (av).

Comparison of the $[Co_3Cp^*_{3-x}Cp'_x(\mu_3\text{-}CO)(\mu_3\text{-}NH)]^n$ Series ($x = 0$, $n = 0, +1$; $x = 1$, $n = 0, +1$; $x = 2$, $n = 0, +1$) with Other Electron-Deficient Homonuclear Trimetal Clusters. Much work has been done to characterize the redox-generated variations in the geometries of triangular metal clusters. Practically all of this research has involved electron-rich systems with only a very few studies of electron-deficient triangular metal clusters.

Theoretical calculations by Hoffmann and co-workers[10] in 1980 on the hypothetical 46-electron $Rh_3Cp_3(\mu_3\text{-}CO)_2$ predicted that such a molecule should possess two unpaired electrons in two doubly degenerate, half-filled e″ HOMOs under D_{3h} symmetry: it was proposed that $Rh_3Cp_3(\mu_3\text{-}CO)_2$ could remain high spin under 3-fold symmetry or undergo a geometrical distortion to break the orbital degeneracy. Possible molecular distortions could occur as the result of a lengthening or contracting of one of the metal–metal bonds, a movement of the triply bridging carbonyls toward a doubly bridging position, and/or a deformation of the Cp rings.

Subsequently, syntheses and structural determinations were reported for the 46-electron $Co_3Cp^*_3(\mu_3\text{-}CO)_2$ (**4**),[3-5] $Co_3Cp_3(\mu_3\text{-}CO)_2$ (**5**),[6] and $Rh_3Cp^*_3(\mu_3\text{-}CO)_2$.[5,7] To our knowledge these are the only crystallographically characterized electron-deficient homonuclear triangular metal clusters containing equivalent ligands per metal atom. Variable-temperature magnetic susceptibility measurements of $Co_3Cp^*_3(\mu_3\text{-}CO)_2$, which possesses crystallographic C_{3h}-3/m site symmetry, established that in the solid state this molecule does not have two unpaired electrons as predicted under assumed 3-fold symmetry. The sizes, shapes, and orientations of the atomic thermal ellipsoids of the $Co_3(CO)_2$ core appear to be normal, with no evidence of being a 3-fold composite of a substantially deformed core of either C_{2v} or C_s symmetry; thus, it was hypothesized[4] that the relatively low magnetic moment of 0.97 μ_B at 280 K in the solid state arises primarily from instantaneous deformations (of non-3-fold molecular symmetry) of the Cp* rings from regular pentagonal symmetry such that the resulting nonequivalent cobalt atoms lift the degeneracy of the two half-filled e″ HOMOs. A low-temperature X-ray diffraction examination[5] of $Rh_3Cp^*_3(\mu_3\text{-}CO)_2$ revealed that its diamagnetism arises from the $Rh_3(CO)_2$ core of crystallographic C_1-1 site symmetry being markedly distorted from an idealized D_{3h} geometry to a C_{2v} geometry with one long and two short Rh–Rh bonds [2.639 (2) Å vs 2.562 Å (av)] and with two long and four short Rh–CO bonds [2.345 Å (av) vs 1.985 Å (av)]. These geometrical differences between the tricobalt and trirhodium structures were attributed[4] to the much stronger metal–metal-bonding interactions for the rhodium atoms as compared to the cobalt atoms.

The 46-electron $Co_3Cp_3(\mu_3\text{-}CO)_2$ (**5**) was recently isolated and structurally characterized by Barnes et al.[6] This molecule also has crystallographic C_{3h}-3/m site symmetry, which results in an averaged structure containing an equilateral cobalt triangle. This averaged structure thereby masks any individual distortions in the $Co_3(CO)_2$ core. The observed Co–Co distance of 2.390 (1) Å is only 0.01 Å shorter than that of 2.399 Å (av) in the 48-electron $[Co_3(\eta^6\text{-}C_6H_6)_3(\mu_3\text{-}CO)_2]^+$ monocation.[3,28] In fact, Barnes et al.[6] suggested that one reason for the unexpectedly long Co–Co distance in **5** may be the high-spin nature of the cobalt cluster. Solution magnetic susceptibility measurements[6] of $Co_3Cp_3(\mu_3\text{-}CO)_2$ via the Evans method gave a magnetic moment of 3.0 μ_B, indicating two unpaired electrons in the two doubly degenerate half-filled e″ HOMOs under D_{3h} symmetry.[3,10] However, solid-state magnetic susceptibility measurements of this molecule indicated possible diamagnetic behavior below 100 K, such that the electronic ground state may actually be a singlet.[6]

(28) (a) Chini, P.; Ercoli, R. *Gazz. Chim. Ital.* **1958**, *88*, 1170–1182. (b) Fischer, E. O.; Beckert, O. *Angew. Chem.* **1958**, *70*, 744.

Of particular interest is that prior to its synthesis, a 0.025-Å shorter Co–Co distance than that of 2.370 (1) Å found[4] in $Co_3Cp^*_3(\mu_3\text{-}CO)_2$ (**4**) had been predicted for **5** under the assumption that the Cp* ligands in **4** would sterically increase its *mean* Co–Co distance by ca. 0.025 Å.[3] This prediction was based upon a comparison of the mean Co–Co bond length in the 46-electron **4** with those in eight other 48-electron $[Co_3(\eta^5\text{-}C_5R_5)_3(\mu_3\text{-}X)(\mu_3\text{-}Y)]^n$ clusters containing Co_3XY cores (for which X = CO, CS, NO; Y = O, NO, NR, S) with either Cp(four), Cp′(three), or Cp*(one) ligands. It was found both in **4** and in six of the seven bicapped triangular cobalt clusters containing sterically innocent Cp or Cp′ ligands that the mean Co–Co distance correlates with the size of the larger capping atom of the triply bridging X and Y ligands and is relatively insensitive to whether the π-acceptor capping ligand is CO, NO, or CS. The fact that the mean Co–Co distance of 2.399 Å for the benzene-coordinated $Co_3(CO)_2$ core of the 48-electron $[Co_3(\eta^6\text{-}C_6H_6)_3(\mu_3\text{-}CO)_2]^+$ is virtually identical with the mean Co–Co distances of 2.399–2.406 Å for the four Cp- or Cp′-coordinated tricobalt clusters with similar-sized C,N- or N,N-bicapping atoms led to the conclusion that the benzene ligands as well as the Cp and Cp′ ligands are sterically innocent.[3] The presumed steric noninnocence of the Cp* ligands in **4** was suggested from the mean Co–Co distance in the 48-electron **1** being 0.025 Å larger than those in the other two 48-electron Cp′-coordinated $Co_3(CO)(NR)$ cores [R = H; R = $C(O)NH_2$]. These bond-length arguments coupled with a theoretical analysis[3] of $Co_3Cp_3(\mu_3\text{-}CO)_2$ via the Fenske–Hall model[15] formed the basis for our conclusion "that the transformation of an electron-deficient 46-electron $M_3(CO)_2$ core to a normal 48-electron one involves a "net" destabilization of the relatively weak metal–metal interactions which are counterbalanced by a "net" stabilization of the much stronger trimetal-carbonyl interactions".[3]

The analysis of the 47-electron tricobalt clusters presented herein emphasize that the replacement of a Cp* ligand by a Cp′ (or Cp) ligand has an important electronic effect. It significantly alters the Co–CO distances and, in conjunction with concomitant changes in the Co–C(O)–Co bond angles, plays a major role in determining the Co–Co distances. especially those in electron-deficient clusters in which the HOMOs contain a large trimetal–carbonyl bonding component. Its extension to the isostructral 46-electron $Co_3Cp^*_3(\mu_3\text{-}CO)_2$ (**4**) and $Co_3Cp_3(\mu_3\text{-}CO)_2$ (**5**) provides an explanation (i.e., weaker Co–CO π back-bonding) for the 0.022-Å larger Co–CO distance in **5** compared to that in **4**. The shorter Cp*Co–CO distance of 1.951 (6) Å in $Co_3Cp^*_3(\mu_3\text{-}CO)_2$ (**4**) is associated with a shorter Cp*Co–CoCp* distance of 2.370 (1) Å due to the Cp*Co–C(O)–CoCp* bond angle of 74.8°, whereas the longer CpCo–CO distance of 1.973 (4) Å in $Co_3Cp_3(\mu_3\text{-}CO)_2$ (**5**) is also associated with a longer CpCo–CoCp distance of 2.390 (1) Å due to the CpCo–C(O)–CoCp bond angle of 74.6°. The similarity of these bond angles, which are in the middle region of the 71.1–78.6° range found in **1**, $\mathbf{1}^+$, $\mathbf{2}^+$, **3**, and $\mathbf{3}^+$, points to the unexpectedly long Co–Co distance in **5** being due to an unusual electronic effect. Hence, we concur with Barnes et al.[6] that the abnormally long Co–Co distance is crystalline **5** at room temperature is probably due to this tricobalt cluster possessing a triplet state with two unpaired electrons.

Comparison of Electron-Rich and Electron-Deficient Bicapped Tricobalt Clusters. In assessing the geometrical changes that occur upon oxidation and/or reduction of various 48-electron bicapped tricobalt clusters, it becomes clear that reduction to the corresponding 49-electron cluster causes much larger changes in the Co–Co distances than oxidation to a 47- or 46-electron system. Two typical 48/49-electron series that have been crystallographically characterized are the $[Co_3Cp'_3(\mu_3\text{-}NO)(\mu_3\text{-}NH)]^n$ series ($n = +1, 0$)[22] and the $[Co_3Cp'_3(\mu_3\text{-}NO)_2]^n$ series ($n = 0, -1$).[23] Upon reduction of the 48-electron $[Co_3Cp'_3(\mu_3\text{-}NO)(\mu_3\text{-}NH)]^+$ monocation[8] to its 49-electron neutral analogue, the mean Co–Co bond length increases by 0.06 Å (with virtually no change in the mean Co–NO distance) and the $Co_3(NO)(NH)$ core exhibits a distinct Jahn–Teller distortion that lowers the symmetry from an idealized C_{3v} to C_s.[22] This geometrical de-

formation, which involves one Co–Co distance being 0.134 Å longer than the average of the other two Co–Co distances, was rationalized in terms of a first-order Jahn–Teller effect due to the added electron breaking the degeneracy of two e HOMOs (under C_{3v} symmetry). A geometrical comparison of the 49-electron $[Co_3Cp'_3(\mu_3\text{-}NO)_2]^-$ monoanion to its 48-electron neutral parent shows that the increased mean Co–Co bond length of 0.045 Å with no marked geometrical distortion of the monoanion core is entirely consistent with the unpaired electron occupying a nondegenerate a_2' in-plane trimetal antibonding orbital instead of the doubly degenerate e'' orbital (under D_{3h} symmetry). Also noteworthy is that the mean Co–NO bond length of 1.86 Å is the same in both the 48- and 49-electron systems.[23]

This bonding analysis stresses that the bond-length variations in the relatively weak Co–Co bonds in electron-deficient tricobalt clusters containing a capping carbonyl are largely determined by concomitant bond-length changes in the much stronger Co–CO bonds. The observed larger alterations in the Co–CO distances upon oxidation of the 48-electron parents to the electron-deficient 47-electron species points to their HOMOs containing a large component of trimetal–carbonyl bonding character.

This bonding model represents an extension of an explanation by Cirjak, Ginsburg, and Dahl[25] that in the oxidation of the 33-electron $[Co_2Cp^*_2(\mu_2\text{-}CO)_2]^-$ monoanion to its 32-electron neutral parent the observed small *decrease* in the Co–Co distance "may be readily described to the simultaneously *increase* in the lengths of the Co–CO bonds, which in being much stronger than the Co–Co interactions are the dominant factor in opposing any decrease in the Co–Co distance". Since the imposed symmetry of the dimetal antibonding HOMO in the monoanion precludes any carbonyl orbital character for a planar $Co_2(CO)_2$ core, they proposed that the observed increase in the Co–CO bond distances upon oxidation of the $[Co_2Cp^*_2(\mu_2\text{-}CO)_2]^-$ monoanion is due to a "loss of negative charge, which in turn lowers the metal AOs relative to the π^*(CO) symmetry orbitals and thereby decreases the $d\pi(M)\text{–}\pi^*$ (CO) back-bonding". This explanation was subsequently generalized by Bottomley[29] in his bonding assessment of the structural variations of a wide variety of carbonyl- and nitrosyl-bridged metal dimers. Bottomley[29] concluded that the metal–metal distances in carbonyl-bridged dimers are determined mainly by the M–CO distances and the M–C(O)–M bond angles. He also generalized that "the higher the energy of the metal atomic orbitals, the shorter the metal–NO or metal–CO distance" and pointed out that with one exception[30] this rule appears to work well.

Similar π back-bonding arguments were used to rationalize the Co–CO bond lengths being shorter than the Ni–CO bond lengths in the $CoNi_2(CO)_2$ core of the 48/49-electron $[Cp^*CoNi_2Cp_2\text{-}(\mu_3\text{-}CO)_2]^n$ series ($n = 0, -1$).[31,32] The $CoNi_2(CO)_2$ core in the neutral 48-electron cobalt–dinickel molecule conforms within experimental error to C_{2v}-2*mm* symmetry with a considerably shorter Ni–Ni bond length of 2.326 (2) Å relative to two equivalent Co–Ni bond lengths of 2.371 Å (av.)[31] The mean length of 2.356 Å for the three metal–metal bonds is virtually identical with that of 2.358 (2) Å previously found for the metal–metal bonds in the averaged structure of $CoNi_2Cp_3(\mu_3\text{-}CO)_2$. The one-electron reduction of $Cp^*CoNi_2Cp_2(\mu_3\text{-}CO)_2$ to its 49-electron monoanion enlarged the Ni–Ni bond by 0.062 Å to 2.388 (2) Å and the two equivalent Co–Ni bonds by 0.021 Å to 2.392 Å (av); the resulting mean of 2.390 Å is experimentally the same as that of 2.389 (2) Å found for the three crystallographically identical Ni–Ni bond lengths in the 49-electron Fischer–Palm $Ni_3Cp_3(\mu_3\text{-}CO)_2$, in which the unpaired electron occupies an in-plane, trimetal antibonding HOMO of nondegenerate a_2' representation under D_{3h} symmetry.[30,31] The fact that the mean bond lengths in these 48/49-electron cobalt–dinickel clusters are different from those in the 48/49-electron tricobalt clusters illustrates the problem in comparing metal–metal distances among electronically equivalent trimetal clusters with different metal atoms. For this reason, we have restricted our bond-length analysis to closely related tricobalt clusters.

EPR Results for the 47-Electron 1^+ and 2^+. The lack of an EPR signal for the 47-electron 1^+ and 2^+ at room temperature down to 100 K is consistent with there being only a very small splitting of the degenerate e HOMOs upon oxidation of neutral 48-electron **1** and **2** to 1^+ and 2^+, respectively. This close-energy separation of the two orbitals would cause a broadening of the expected signal due to rapid electron-spin relaxation. This effect was observed by Enoki et al.[33] in the electrochemically generated 47-electron $[Co_3Cp_3(\mu_3\text{-}CPh)_2]^+$ monocation, which exhibits a broad signal without any resolved hyperfine structure at 77 K.

Acknowledgment. This research was supported by the National Science Foundation. M.S.Z. is especially grateful to a former co-worker, Dr. Robert L. Bedard, for his assistance in the initial phases of this work. Special thanks are extended to Professor Brock Spencer (Beloit College) for his assistance in performing the EPR measurements. We are also indebted to Mr. Randy K. Hayashi for his help in the crystallographic refinements and in the preparation of this manuscript.

Supplementary Material Available: Twenty-four tables listing parameters for the non-hydrogen atoms, anisotropic thermal parameters, interatomic distances, bond angles, and parameters for the hydrogen atoms (26 pages); observed and calculated structure factor amplitudes for $[Co_3Cp^*_3(\mu_3\text{-}CO)(\mu_3\text{-}NH)]^+[PF_6]^-$, $[Co_3Cp^*_2Cp'(\mu_3\text{-}CO)(\mu_3\text{-}NH)]^+[PF_6]^-$, $Co_3Cp^*Cp'_2(\mu_3\text{-}CO)(\mu_3\text{-}NH)$, and $[Co_3Cp^*Cp'_2(\mu_3\text{-}CO)(\mu_3\text{-}NH)]^+[PF_6]^-$ (61 pages). Ordering information is given on any current masthead page.

(29) Bottomley, F. *Inorg. Chem.* **1983**, *22*, 2656–2660.
(30) See ref 2b for a recent structural-bonding analysis of the presumed exception.
(31) Byers, L. R.; Uchtman, V. A.; Dahl, L. F. *J. Am. Chem. Soc.* **1981**, *103*, 1942–1951.
(32) Maj, J. J.; Rae, A. D.; Dahl, L. F. *J. Am. Chem. Soc.* **1982**, *104*, 3054–3063.
(33) Enoki, S.; Kawamura, T.; Yonezawa, T. *Inorg. Chem.* **1983**, *22*, 3821–3824.